Separated Response Function Ratios in Exclusive, Forward $\pi^{\pm}$ Electroproduction

G.M. Huber,[1] H.P. Blok,[2,3] C. Butuceanu,[1] D. Gaskell,[4] T. Horn,[5] D.J. Mack,[4] D. Abbott,[4] K. Aniol,[6] H. Anklin,[7,4] C. Armstrong,[8] J. Arrington,[9] K. Assamagan,[10] S. Avery,[10] O.K. Baker,[10,4] B. Barrett,[11] E.J. Beise,[12] C. Bochna,[13] W. Boeglin,[7] E.J. Brash,[1] H. Breuer,[12] C.C. Chang,[12] N. Chant,[12] M.E. Christy,[10] J. Dunne,[4] T. Eden,[4,14] R. Ent,[4] H. Fenker,[4] E.F. Gibson,[15] R. Gilman,[16,4] K. Gustafsson,[12] W. Hinton,[10] R.J. Holt,[9] H. Jackson,[9] S. Jin,[17] M.K. Jones,[8] C.E. Keppel,[10,4] P.H. Kim,[17] W. Kim,[17] P.M. King,[12] A. Klein,[18] D. Koltenuk,[19] V. Kovaltchouk,[1] M. Liang,[4] J. Liu,[12] G.J. Lolos,[1] A. Lung,[4] D.J. Margaziotis,[6] P. Markowitz,[7] A. Matsumura,[20] D. McKee,[21] D. Meekins,[4] J. Mitchell,[4] T. Miyoshi,[20] H. Mkrtchyan,[22] B. Mueller,[9] G. Niculescu,[23] I. Niculescu,[23] Y. Okayasu,[20] L. Pentchev,[8] C. Perdrisat,[8] D. Pitz,[24] D. Potterveld,[9] V. Punjabi,[14] L.M. Qin,[18] P.E. Reimer,[9] J. Reinhold,[7] J. Roche,[4] P.G. Roos,[12] A. Sarty,[11] I.K. Shin,[17] G.R. Smith,[4] S. Stepanyan,[22] L.G. Tang,[10,4] V. Tadevosyan,[22] V. Tvaskis,[2,3] R.L.J. van der Meer,[1] K. Vansyoc,[18] D. Van Westrum,[25] S. Vidakovic,[1] J. Volmer,[2,26] W. Vulcan,[4] G. Warren,[4] S.A. Wood,[4] C. Xu,[1] C. Yan,[4] W.-X. Zhao,[27] X. Zheng,[9] and B. Zihlmann[28,4]

(The Jefferson Lab F_π Collaboration)

[1] *University of Regina, Regina, Saskatchewan S4S 0A2, Canada*
[2] *VU university, NL-1081 HV Amsterdam, The Netherlands*
[3] *NIKHEF, Postbus 41882, NL-1009 DB Amsterdam, The Netherlands*
[4] *Physics Division, TJNAF, Newport News, Virginia 23606*
[5] *Catholic University of America, Washington, DC 20064*
[6] *California State University Los Angeles, Los Angeles, California 90032*
[7] *Florida International University, Miami, Florida 33119*
[8] *College of William and Mary, Williamsburg, Virginia 23187*
[9] *Physics Division, Argonne National Laboratory, Argonne, Illinois 60439*
[10] *Hampton University, Hampton, Virginia 23668*
[11] *Saint Mary's University, Halifax, Nova Scotia, Canada*
[12] *University of Maryland, College Park, Maryland 20742*
[13] *University of Illinois, Champaign, Illinois 61801*
[14] *Norfolk State University, Norfolk, Virginia*
[15] *California State University, Sacramento, California 95819*
[16] *Rutgers University, Piscataway, New Jersey 08855*
[17] *Kyungpook National University, Taegu, Korea*
[18] *Old Dominion University, Norfolk, Virginia 23529*
[19] *University of Pennsylvania, Philadelphia, Pennsylvania 19104*
[20] *Tohoku University, Sendai, Japan*
[21] *New Mexico State University, Las Cruces, New Mexico 88003-8001*
[22] *Yerevan Physics Institute, 375036 Yerevan, Armenia*
[23] *James Madison University, Harrisonburg, Virginia 22807*
[24] *DAPNIA/SPhN, CEA/Saclay, F-91191 Gif-sur-Yvette, France*
[25] *University of Colorado, Boulder, Colorado 76543*
[26] *DESY, Hamburg, Germany*
[27] *M.I.T.–Laboratory for Nuclear Sciences and Department of Physics, Cambridge, Massachusetts 02139*
[28] *University of Virginia, Charlottesville, Virginia 22901*

(Dated: May 22, 2013)

The study of exclusive $\pi^{\pm}$ electroproduction on the nucleon, including separation of the various structure functions, is of interest for a number of reasons. The ratio $R_L = \sigma_L^{\pi^-}/\sigma_L^{\pi^+}$ is sensitive to isoscalar contamination to the dominant isovector pion exchange amplitude, which is the basis for the determination of the charged pion form factor, $F_\pi(Q^2)$, from electroproduction data. A change in the value of $R_T = \sigma_T^{\pi^-}/\sigma_T^{\pi^+}$ from unity at small $-t$, to 1/4 at large $-t$, would suggest a transition from coupling to a (virtual) pion to coupling to individual quarks. Furthermore, the mentioned ratios may show an earlier approach to pQCD than the individual cross sections. Here, we report on the first complete separation of the four unpolarized electromagnetic structure functions above the dominant resonances in forward, exclusive $\pi^{\pm}$ electroproduction on the nucleon at central Q^2 values of 0.6, 1.0, 1.6 GeV^2 at W=1.95 GeV, and Q^2 = 2.45 GeV^2 at W=2.22 GeV. Results for the separated ratio R_L indicate dominance of the pion-pole diagram at low $-t$, while results for R_T are consistent with a transition between pion knockout and quark knockout mechanisms.

PACS numbers: 14.40.Aq,13.40.Gp,13.60.Le,25.30.Rw,11.55.Jy

Measurements of exclusive meson production are a useful tool in the study of hadronic structure. Through these studies, one can discern the relevant degrees of freedom at different distance scales. In contrast to inclusive (e, e') or photoproduction measurements, the transverse momentum (size) of a scattering constituent and the resolution at which it is probed can be varied independently. Exclusive *forward pion* electroproduction is especially interesting, because by detecting the charge of the pion, even the flavor of the constituents can be tagged. Finally, *ratios* of separated response functions can be formed for which nonperturbative corrections may cancel, yielding insight into soft-hard factorization at the modest Q^2 to which exclusive measurements will be limited for the foreseeable future.

The longitudinal response in exclusive charged pion electroproduction has several important applications. At low $-t$ and nearly arbitrary Q^2, it can be related to the charged pion form factor, $F_\pi(Q^2)$, [1] which is used to test non-perturbative models of this "positronium" of light quark QCD. In order to reliably extract F_π from electroproduction data, the isovector t-pole process should be dominant in the kinematic region under study. This dominance can be studied experimentally through the ratio of longitudinal $\gamma_L^* n \to \pi^- p$ and $\gamma_L^* p \to \pi^+ n$ cross sections, because G-parity conservation restricts t-channel exchanges to $G = +1$ and -1 for the respective isoscalar and isovector photon amplitudes. Thus, if the photon possessed definite isospin, exclusive π^- production on the neutron and π^+ production on the proton would be related to each other by simple isospin rotation and the cross sections would be equal [2]. A departure from $R_L \equiv \sigma_L^{\pi^-}/\sigma_L^{\pi^+} = 1$ would indicate the presence of isoscalar backgrounds arising from mechanisms such as ρ meson[3] or contributions due to transverse quark momentum[4]. Such physics backgrounds may be expected to be larger at higher $-t$ (due to the drop-off of the pion pole) or non-forward kinematics (due to angular momentum conservation). Because previous data are unseparated [5], no firm conclusions about possible deviations of R_L from unity are possible.

At low $-t$, also the transverse ratio $R_T = \frac{\gamma_T^* n \to \pi^- p}{\gamma_T^* p \to \pi^+ n}$ is expected to be near unity, as the photon is supposed to couple to the charge of the pion. With increasing $-t$, the photon starts to probe quarks rather than pions, and the charge of the produced pion acts as a tag on the flavor of the participating constituent. Applying isospin decomposition and charge symmetry invariance to s-channel knockout of valence quarks in the hard-scattering regime, Nachtmann [8] predicted the exclusive electroproduction π^-/π^+ ratio to be

$$\frac{\gamma_T^* n \to \pi^- p}{\gamma_T^* p \to \pi^+ n} = \left(\frac{e_d}{e_u}\right)^2 = \frac{1}{4}.$$

This prediction applies only to transversely polarized virtual photons, since the absorption of longitudinal virtual photons is a non-asymptotic process in the simple quark-parton model. Previous unseparated π^-/π^+ data[5] trend to a ratio of 1/4 for $|t| > 0.6$ GeV^2, but with relatively large uncertainties.

In the transition region between low momentum transfer (where a description of hadronic degrees of freedom in terms of effective hadronic Lagrangians is valid) and large momentum transfer (where the degrees of freedom are quarks and gluons), t-channel exchange of a few Regge trajectories permits an efficient description of the energy dependence and the forward angular distribution of many real- and virtual-photon-induced reactions. The VGL Regge model [9, 10] has provided a good and consistent description of a wide variety of $\pi^\pm$ photoproduction data above the resonance region, as well as the $p(e, e'\pi^+)n$ reaction using longitudinally polarized virtual photons. However, the model has consistently failed to provide a good description of the $\sigma_{\rm T}$ data from this reaction [11]. The VGL Regge model was recently extended [12] by the addition of a hard deep inelastic scattering (DIS) process of virtual photons off nucleons. The DIS process dominates the transverse response at moderate and high Q^2, providing a better description of $\sigma_{\rm T}$.

We have performed a complete L/T/LT/TT separation in exclusive forward $\pi^\pm$ electroproduction from deuterium. Here, we present the L and T cross sections, with emphasis on R_L and R_T in order to better understand the dynamics of this fundamental inelastic process. Because there are no practical free neutron targets, the ^{2}H$(e, e'\pi^\pm)NN_s$ reactions (where N_s denotes the spectator nucleon) were used. In π^-/π^+ ratios, the corrections for nuclear binding and rescattering largely cancel. The data were obtained in Hall C at the Thomas Jefferson National Accelerator Facility (JLab) as part of the two pion form factor experiments presented in detail in Ref. [11]. Except where noted, the experimental details and data analysis techniques are as presented in Ref. [11] for the ^{1}H$(e, e'\pi^+)n$ data. Charged $\pi^\pm$ were detected in the High Momentum Spectrometer (HMS) while the scattered electrons were detected in the Short Orbit Spectrometer (SOS). Given the kinematic constraints imposed by the available electron beam energies and the properties of the HMS and SOS magnetic spectrometers, deuterium data were acquired in the first experiment for nominal Q^2, W, $\Delta\epsilon$ settings of $(0.60, 1.95, 0.37)$, $(1.00, 1.95, 0.32)$, $(1.60, 1.95, 0.36)$, and in the second experiment of $(2.45, 2.22, 0.27)$. The W=1.95 GeV used in the first experiment is high enough to suppress most s-channel baryon resonance backgrounds, but this suppression should be even more effective in the second experiment. For each Q^2 setting, the electron spectrometer angle and momentum, as well as the pion spectrometer momentum, were kept fixed. To attain full coverage in ϕ, additional data were taken with the pion spectrometer at a slightly smaller and a larger angle than the $\vec{q}$-vector direction for the high ϵ settings. At low ϵ, only the larger angle setting was possible.

The HMS magnetic polarity was reversed between π^+ and π^- running, with the quadrupoles and dipole magnets cycled according to a standard procedure. Kinematic offsets in spectrometer angle and momentum, as well as in beam energy, were previously determined using elastic e^-p coincidence data taken during the same run [11]. The reproducibility of the optics was checked during electron running with sieve slits and by the position of the missing mass peak for $^2\mathrm{H}(e,e'\pi^+)nn_s$ or $^2\mathrm{H}(e,e'\pi^-)pp_s$. No shifts beyond the expected calibration residuals ± 2 MeV were observed.

Once the detectors were calibrated, particle identification was established in each spectrometer. The potential contamination by electrons when the pion spectrometer is set to negative polarity, and by protons when it is set to positive polarity, introduces asymmetries in the $\pi^\pm$ data analyses which were treated very carefully. For most negative HMS polarity runs, electrons were rejected at the trigger level by a gas Čerenkov detector containing C_4F_{10}. The beam current was significantly reduced during π^- running to minimize the inefficiency due to electrons passing through the gas Čerenkov within ≈ 100 ns after a pion has traversed the detector, causing the pion to be misidentified as an electron. A Čerenkov blocking correction (2-15%) was determined by comparison to runs where the Čerenkov was not in the trigger, and applied to the π^- data where applicable. A cut on particle speed ($\beta > 0.95$), calculated from the time-of-flight difference between two scintillator planes in the HMS detector stack, was applied to separate π^+ from protons. Additionally in the second experiment, an aerogel Čerenkov detector was used to separate protons and π^+ for central momenta above 3 GeV/c. A correction for the number of pions lost (2.5-5%), due to pion nuclear interactions in the HMS detector stack, was determined from the π^- data. To account for lost triggers due to pion absorption in the HMS vacuum window, drift chambers and first scintillator plane, an additional pion absorption correction ($1 \pm 1\%$ for the first experiment and $2 \pm 1\%$ for the second experiment) was applied. For further details, see Ref. [11].

Because the π^- data are typically taken at higher HMS detector rates than the π^+ data, a good understanding of rate dependent detector efficiency corrections was also required. An improved high rate tracking algorithm was implemented, resulting in high rate tracking inefficiencies of 2-9% for HMS rates up to 1.4 MHz. Conversely, the lower detector rates when the HMS was set at positive polarity meant that higher incident electron beam currents were often used for the π^+ runs. Liquid deuterium target boiling corrections of 4.7%/100 μA were determined for the horizontal-flow target used in the first experiment. The vertical-flow target and improved beam raster used in the second experiment resulted in a negligible boiling correction for those data. In addition to the above corrections, the experimental yields were also corrected for computer dead time (1-11%).

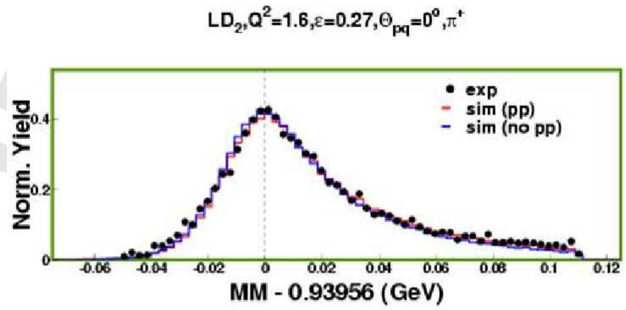

FIG. 1. (Color online) Missing mass of the undetected nucleon calculated as quasi-free pion electroproduction. In addition to the experimental data, quasi-free Monte Carlo simulations with and without the effect of pions penetrating the HMS collimator are shown. This addition resulted in an overall improvement in all simulated kinematic variables in comparison to the experimental data, allowing the missing mass region 0.875¡MM¡1.03 GeV to be used in the analysis.

Kinematic quantities such as the Mandelstam variable t and the missing mass MM were reconstructed as quasi-free pion electroproduction, $\gamma_v N \rightarrow \pi^\pm N'$, where the virtual photon interacts with a nucleon at rest. The former is calculated using $t = (p_{target} - p_{recoil})^2$, which is not necessarily equivalent to $(p_\gamma - p_\pi)^2$ due to Fermi momentum and radiation. Missing mass cuts were then applied to select the exclusive final state. Because of Fermi momentum in the deuteron, this cut ($0.875 \leq MM \leq 1.03$ GeV) is taken wider than for hydrogen. The MM cut upper limit was determined by the value where the missing mass peak is no longer well reproduced by a quasi-free Monte Carlo simulation including all known detector effects (Fig. 1), indicating the presence of additional backgrounds, such as two pion production. Real and random coincidences were isolated with a coincidence time cut of ± 1 ns. The randoms were subtracted on a bin by bin basis. Background from aluminum target cell walls (2-4% of the yield) and random coincidences ($\sim 1\%$) were also subtracted from the charge normalized yields. Compared to hydrogen, the backgrounds from target windows and random coincidences are generally larger due to the wider MM cut.

Following our earlier procedure [11], we write the unpolarized pion electroproduction as the product of a virtual photon flux factor and a virtual photon cross section,

$$\frac{d^5\sigma}{d\Omega_e dE_e' d\Omega_\pi} = J\left(t,\phi \rightarrow \Omega_\pi\right) \Gamma_v \frac{d^2\sigma}{dt d\phi}, \qquad (1)$$

where $J\left(t,\phi \rightarrow \Omega_\pi\right)$ is the Jacobian of the transformation from $dtd\phi$ to $d\Omega_\pi$, ϕ is the azimuthal angle between the scattering and the reaction plane, and

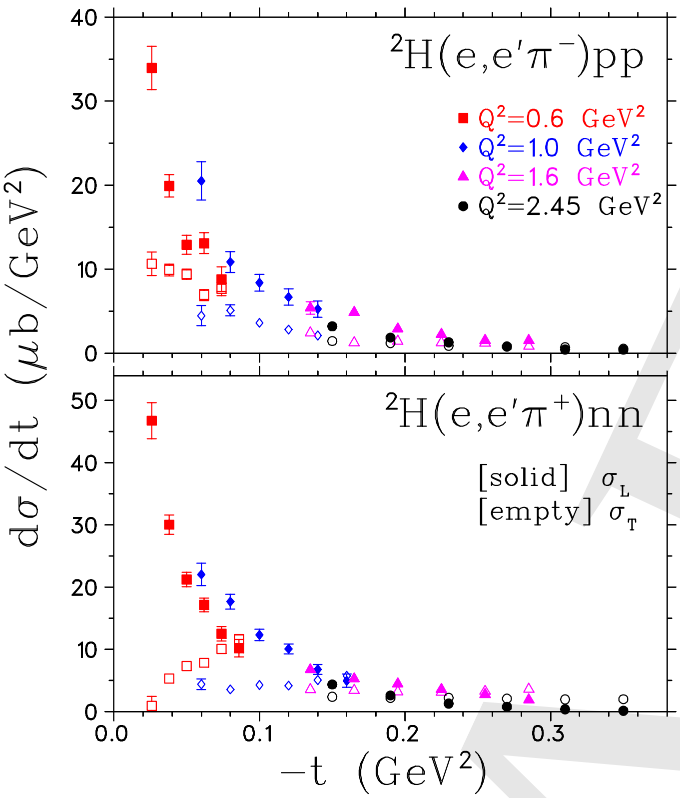

FIG. 2. (Color online) Separated exclusive $\pi^{\pm}$ electroproduction cross sections from deuterium at nominal values of Q^2. Because the data were taken at different values of $\overline{W}$, all cross sections were scaled to a value of $W = 2.0$ GeV according to $1/(W^2 - M^2)$. The error bars indicate statistical and uncorrelated systematic uncertainties in both ϵ and $-t$, combined in quadrature.

$\Gamma_v = \frac{\alpha}{2\pi^2}\frac{E_e'}{E_e}\frac{1}{Q^2}\frac{1}{1-\epsilon}\frac{W^2-M^2}{2M}$ is the virtual photon flux factor. The virtual photon cross section can be expressed in terms of contributions from transversely and longitudinally polarized photons,

$$2\pi\frac{d^2\sigma}{dt d\phi} = \frac{d\sigma_T}{dt} + \epsilon\frac{d\sigma_L}{dt} + \sqrt{2\epsilon(1+\epsilon)}\frac{d\sigma_{LT}}{dt}cos\phi \quad (2)$$
$$+ \epsilon\frac{d\sigma_{TT}}{dt}cos2\phi.$$

Here, $\epsilon = \left(1 + 2\frac{|\vec{q}|^2}{Q^2}\tan^2\frac{\theta}{2}\right)^{-1}$ is the virtual photon polarization, where $\vec{q}$ is the three-momentum transferred to the quasi-free nucleon and θ is the electron scattering angle.

For each charge state, the data for $d^2\sigma/dtd\phi$ were binned in t and ϕ and the individual components in Eqn. 2 determined from a simultaneous fit to the ϕ dependence of the measured cross sections at two values of ϵ. The separated cross sections are determined at fixed values of W, Q^2, common for both high and low values of ϵ. Because the acceptance covers a range in W and Q^2, the measured cross sections, and hence the separated response functions, represent an average over this range. They are determined at the average values (for both ϵ points together), $\overline{Q}^2$, $\overline{W}$, which are different for each t bin. In order to minimize errors resulting from averaging, the experimental cross sections were calculated by comparing the experimental yields to a Monte Carlo simulation of the experiment. The simulation uses a quasi-free $N(e, e'\pi^{\pm})N'$ model, where the struck nucleon carries Fermi momentum, but the events are reconstructed in the same manner as the experimental data, i.e. assuming the target is a nucleon at rest. The Monte Carlo includes a detailed description of the spectrometers, multiple scattering, ionization energy loss, pion decay, and radiative processes.

Due to the fact that the Monte Carlo and bin-centering model ignores any potential off-shell effects, the extracted separated cross sections are effective ones, not directly comparable to those from ^{1}H. We believe it is better that the influence of off-shell (and possible other mechanisms in ^{2}H) are studied separately, using cross sections that are determined in a well-defined way, than that off-shell effects are incorporated already in some way in the extracted cross sections (although the differences in practice may not be large). The separated cross sections, σ_{L} and σ_{T}, are shown in Fig. 2. The uncertainties in the separated cross sections have both statistical and systematic sources. The statistical uncertainty in $\sigma_T + \epsilon\sigma_L$ is 5-10% for π^- settings, and more uniformly near 5% for π^+ settings. Systematic uncertainties that are uncorrelated between high and low ϵ points are amplified by a factor of $1/\Delta\epsilon$ in the L/T separation. This ~1.5% uncertainty is dominated by uncertainties in the spectrometer acceptance, uncertainties in the efficiency corrections due to Čerenkov trigger blocking and analysis cuts, and the Monte Carlo model dependence. Scale systematic uncertainties of 3-4% (not shown in the figure) propagate directly into the separated cross sections. They are dominated by uncertainties in the radiative corrections, pion decay and pion absorption corrections, and the tracking efficiencies.

In the L response of Fig. 2, the pion pole is evident by the sharp rise at small $-t$. π^- and π^+ are similar, and the data at different Q^2 follow a nearly universal curve versus t, with only a weak Q^2-dependence. The T responses are flatter versus t, and with the exception of the $Q^2 = 0.6$ GeV^2 π^+ data, also follow a nearly universal curve.

Finally, π^-/π^+ ratios of the separated cross sections were formed to cancel nuclear binding and rescattering effects. Many experimental normalization factors cancel to a high degree in the ratio (acceptance, target thickness, pion decay and absorption in the detectors, radiative corrections, etc.). The principal remaining uncorrelated systematic errors are in the tracking inefficiencies, target boiling corrections, Čerenkov blocking corrections, and statistics.

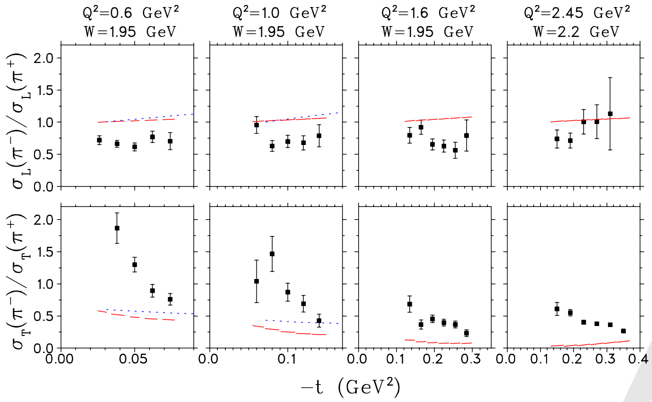

FIG. 3. (Color online) The ratios $R_L \equiv \sigma_L^{\pi^-}/\sigma_L^{\pi^+}$ and $R_T \equiv \sigma_T^{\pi^-}/\sigma_T^{\pi^+}$ versus $-t$ for four Q^2 settings. The error bars include statistical and uncorrelated systematic uncertainties. The dashed red curves are predictions of the VGL Regge model [10] using the values $\Lambda_\pi^2 = 0.405$, 0.503, 0.654, 0.636 GeV^2, as determined from fits to our ^{1}H data [11], and calculated at the same $\overline{W}$, $\overline{Q^2}$ as the data. The dotted blue curves are predictions by Kaskulov and Mosel [12], calculated at the nominal kinematics.

Fig. 3 shows the first determination of R_L above the resonance region. The ratio is approximately 0.8 near $-t_{min}$ at each Q^2 setting. We note that $R_L = 0.8$ was predicted in the large N_c limit calculation of Ref. [13]. The data are lower, especially at the lower values of Q^2 taken also at lower W, than the predictions of the pion-pole dominated models [10, 12]. A simple estimate, under the not necessarily realistic assumption that the isoscalar and isovector amplitudes are real, is that $R_L = 0.8$ is consistent with $|A_S/A_V| = 6\%$. These results indicate that pion exchange dominates the forward longitudinal response even $\sim 10\ m_\pi^2$ away from the pion pole. This is relevant for the extraction of the pion form factor from electroproduction data, which uses a model including some isoscalar background.

Also in Fig. 3 are the first $R_T \equiv \sigma_T^{\pi^-}/\sigma_T^{\pi^+}$ results in electroproduction at high momentum transfers. The behavior of R_T changes dramatically with increasing Q^2 over a fairly small range in $-t$, reaching 0.23-0.27 at larger Q^2 and $-t$. It is interesting to note that this value is reached at a much lower value of $-t$ than for the unseparated ratios of Ref. [5]. A value of $-t = 0.3$ GeV^2 seems quite a low value for quark charge scaling arguments to apply directly. This might indicate the partial cancellation of soft QCD corrections in the formation of the π^-/π^+ ratio. Previous photoproduction measurements of R_T have hinted at quark-partonic behavior [14], but such non-forward, $Q^2 = 0$ measurements are inherently more difficult to interpret due to sea quark and u-channel contributions. Indeed, the photoproduction measurements at sufficiently high $-t$ first dip down toward 1/4 then *increase* at backward angles. The VGL and Kaskulov-Mosel models are unable to accurately predict R_T at $-t_{min}$. Further theoretical work is clearly needed to investigate alternate explanations of the observed ratios.

To summarize, our data for R_L above the resonance region indicate that isoscalar processes dominate in forward kinematics. A small increase in R_L at larger $-t$ is in qualitative agreement with the Regge meson exchange model. The reaction mechanism for the transverse response at our highest $-t$ is consistent with s-channel quark knockout as evidenced by $R_T \simeq 0.25$, possibly indicating the cancellation of soft QCD corrections. Finally, R_L is clearly an experimentally accessible ratio of longitudinal photon observables, and is likely to play an important role in future GPD programs. Further work is planned after the completion of the JLab 12 GeV upgrade, including complete separations at Q^2=5-10 GeV^2 over a larger range of $-t$.

The authors thank Drs. Guidal, Laget, and Vanderhaeghen for stimulating discussions and for modifying their computer program for our needs. This work is supported by DOE and NSF (USA), NSERC (Canada), FOM (Netherlands), NATO, and KOSEF (South Korea). Additional support from Jefferson Science Associates and the University of Regina is gratefully acknowledged. At the time these data were taken, the Southeastern Universities Research Association (SURA) operated the Thomas Jefferson National Accelerator Facility for the United States Department of Energy under contract DE-AC05-84150.

[1] G.M. Huber, et al., Phys. Rev. C **78** (2008) 045203.
[2] A.M. Boyarski et al, Phys. Rev. Lett. **21** (1968) 1767.
[3] M. Vanderhaeghen, M. Guidal, and J.-M. Laget, Phys. Rev. C **57** (1998) 57.
[4] C.E. Carlson, Joseph Milana, Phys. Rev. Lett. **65** (1990) 1717.
[5] P. Brauel *et al.*, Z. Physik C **3**, 101-123 (1979), M. Schaedlich, Dissertation des Doktorgrades, Universitaet Hamburg, 1976, DESY F22-76/02 November 1976.
[6] J.C. Collins, L. Frankfurt, M. Strikman, Phys. Rev. D **56** (1997) 2982.
[7] M.I. Eides, L.L. Frankfurt, M.I. Strikman, Phys. Rev. D **59** (1999) 114025.
[8] O. Nachtmann, Nucl. Phys. **B115** (1976) 61.
[9] M. Guidal, J.-M. Laget, M. Vanderhaeghen, Nucl. Phys. **A 627** (1997) 645.
[10] M. Vanderhaeghen, M. Guidal, J.-M. Laget, Phys. Rev. C **57** (1998) 1454.
[11] H.P. Blok, et al., Phys. Rev. C **78** (2008) 045202.
[12] M.M. Kaskulov, U. Mosel, Phys. Rev. C **81** (2010) 045202.
[13] L.L. Frankfurt, M.V. Polyakov, M. Strikman, M. Vanderhaeghen, Phys. Rev. Lett. **84** (2000) 2589.
[14] L.Y. Zhu, et al., Phys. Rev. Lett. **91** (2003) 022003 (2003); Phys. Rev. C **71** (2005) 044603.